

When Classes Evolve: A Benchmark and Framework for Stage-Aware Class-Incremental Learning

Zheng Zhang ^{*1} Tao Hu ^{*23} Xueheng Li ²³ Yang Wang ²³ Rui Li ³ Jie Zhang ³ Chengjun Xie ³

Abstract

Class-Incremental Learning (CIL) aims to sequentially learn new classes while mitigating catastrophic forgetting of previously learned knowledge. Conventional CIL approaches implicitly assume that classes are morphologically static, focusing primarily on preserving previously learned representations as new classes are introduced. However, this assumption neglects intra-class evolution: a phenomenon wherein instances of the same semantic class undergo significant morphological transformations, such as a larva turning into a butterfly. Consequently, a model must both discriminate between classes and adapt to evolving appearances within a single class. To systematically address this challenge, we formalize Stage-Aware CIL (Stage-CIL), a paradigm in which each class is learned progressively through distinct morphological stages. To facilitate rigorous evaluation within this paradigm, we introduce the Stage-Bench, a 10-domain, 2-stages dataset and protocol that jointly measure inter- and intra-class forgetting. We further propose STAGE, a novel method that explicitly learns abstract and transferable evolution patterns within a fixed-size memory pool. By decoupling semantic identity from transformation dynamics, STAGE enables accurate prediction of future morphologies based on earlier representations. Extensive empirical evaluation demonstrates that STAGE consistently and substantially outperforms existing state-of-the-art approaches, highlighting its effectiveness in simultaneously addressing inter-class discrimination and intra-class morphological adaptation. Source code is available upon acceptance.

¹Dalian University of Technology ²University of Science and Technology of China ³Hefei Institutes of Physical Science, Chinese Academy of Sciences. Correspondence to: Zheng Zhang <ericzhengz@mail.dlut.edu.cn>, Chengjun Xie <cjxie@iim.ac.cn>.

Preprint.

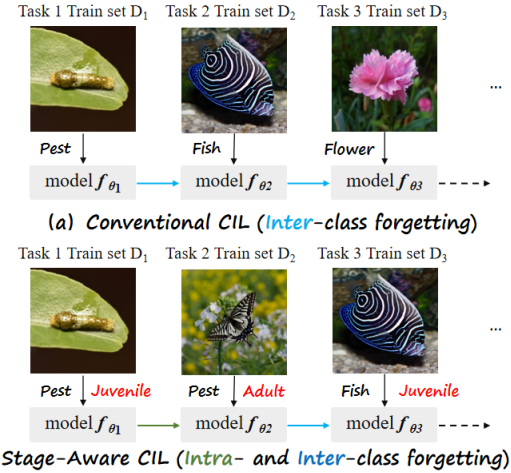


Figure 1. Conventional CIL focuses on inter-class forgetting across distinct categories. Stage-CIL introduces temporally ordered morphological stages within each class, giving rise to the new problem of intra-class forgetting while retaining the original inter-class challenge.

1. Introduction

Intelligent systems deployed in the real world must learn from non-stationary data streams (Shaheen et al., 2022; Wang et al., 2024). Class-Incremental Learning (CIL) (Rebuffi et al., 2017; De Lange et al., 2021) addresses this requirement by sequentially introducing new classes while retaining previously acquired knowledge, yet remains fundamentally constrained by catastrophic forgetting (French, 1999; McCloskey et al., 1989). Contemporary solutions, including replay-based strategies (Choi et al., 2024; Jiang et al., 2025) and PTM-driven modular tuning (Wang et al., 2022c; Sun et al., 2025b; Zhou et al., 2025b), largely follow a common design principle: isolating knowledge across classes to minimize interference. This principle is effective for inter-class discrimination, ensuring that learning "fish" does not erase "butterflies", but implicitly assumes that each class is morphologically static. This assumption often fails in natural and man-made scenarios where a single semantic class undergoes structured and substantial morphological evolution. A larva grows into a butterfly; a new car gradually accumulates damage. Such changes alter the visual

appearance while preserving class identity. Under these conditions, existing CIL methods become misaligned, as they tend to overwrite earlier stages or implicitly fragment one class into separate modules (Fig. 1), yielding a form of intra-class forgetting that standard CIL protocols and metrics cannot characterize. Although this phenomenon bears a superficial resemblance to domain shift (Feng et al., 2024), intra-class evolution is class-conditioned and temporally ordered, rather than externally induced or unconstrained. Evaluating it requires explicit cross-stage supervision and measurements of stage-wise identity coherence, which lie outside the design of current CIL and DIL benchmarks.

We therefore formalize Stage-Aware Class-Incremental Learning (Stage-CIL), a setting where each class is introduced through its evolving morphological stages, combining the classical challenge of inter-class discrimination with the new requirement of maintaining identity across stages. We then construct Stage-Bench, the first multi-domain benchmark tailored for Stage-CIL, spanning 10 diverse domains and providing standardized protocols, evaluation splits, and two diagnostic metrics (Inter/Intra-Class-Forgetting) for quantifying cross-stage forgetting.

To demonstrate that Stage-CIL is both learnable and meaningfully distinct from existing CIL formulations, we further introduce STAGE, a proof-of-concept framework that models stage evolution through a shared set of canonical transformation patterns. Given an early-stage instance, the model predicts its future morphology and aligns this prediction with its ground-truth next stage, yielding a generalizable understanding of class evolution. STAGE is developed primarily to substantiate the Stage-CIL setting, providing strong empirical evidence while also serving as a competitive evolution-aware baseline.

Our contributions are threefold:

- We introduce the Stage-CIL paradigm and its principled protocol, highlighting the previously unmodeled challenge of intra-class evolution within continual learning.
- We release Stage-Bench, a comprehensive benchmark with standardized evaluation tools and diagnostic metrics tailored for this new problem.
- We develop STAGE as a proof-of-concept model, validating that modeling morphological transformation is a promising direction for addressing intra-class forgetting in Stage-CIL.

2. Related Work

2.1. Class-Incremental Learning

Class-Incremental Learning (CIL) studies the problem of learning a sequence of class sets while retaining knowledge

of previously observed classes (Rebuffi et al., 2017). A large amount of research focuses on mitigating catastrophic forgetting (French, 1999), and existing methods can be grouped into several representative paradigms. Distillation-based approaches preserve predictions of earlier models to constrain the learning dynamics of new tasks (Li & Hoiem, 2018; Rebuffi et al., 2017). Rehearsal-based methods maintain a memory buffer of exemplars and periodically replay them to stabilize decision boundaries (Chaudhry et al., 2018). Parameter-regularization techniques such as EWC (Kirkpatrick et al., 2017) restrict the drift of important weights, while model-expansion methods allocate additional sub-networks or task-specific components to reduce interference (Rusu et al., 2017).

With the increasing adoption of Pre-trained Models (PTMs), PTM-based CIL has become a central research direction (Zhou et al., 2024a). These methods typically freeze the backbone and focus on adapting lightweight modules. L2P (Wang et al., 2022c) retrieves instance-specific prompts from a prompt pool, and DualPrompt (Wang et al., 2022b) separates task-invariant and task-specific prompts. CODA-Prompt (Smith et al., 2023) composes decomposed prompts using attention mechanisms, while DAP (Jung et al., 2023) shifts from prompt selection to prompt generation. Adapter-based designs such as MOS (Sun et al., 2025b) introduce task-specific adapters with progressive merging strategies. Prototype-driven approaches, including SimpleCIL (Zhou et al., 2025a), APER (Zhou et al., 2024c), and RanPAC (McDonnell et al., 2023), leverage prototypical classifiers or random projections on top of frozen features, often achieving strong performance with minimal parameter updates.

2.2. Domain-Incremental Learning

Domain-Incremental Learning (DIL) considers scenarios where the label space is fixed but the input distribution varies across domains (van de Ven & Tolias, 2022). The goal is to acquire new domain knowledge while maintaining performance on previously learned domains without explicit task identifiers. Recent work increasingly leverages PTMs for their robustness under distribution shifts. S-Prompts (Wang et al., 2022a) learns a pool of domain-specific prompts and retrieves them using similarity search. DCE (Li et al., 2025) introduces frequency-aware expert networks and a dynamic selector to balance intra- and inter-domain adaptation. Prototype-based or projection-based approaches such as SimpleCIL (Zhou et al., 2025a) and RanPAC (McDonnell et al., 2023) have also demonstrated strong cross-domain performance due to their minimal reliance on updated parameters.

While both CIL and DIL address non-stationary learning, they operate under different structural assumptions: CIL focuses on sequentially expanding the label space, whereas

DIL models domain-wise distribution shifts under a fixed label space. These perspectives provide complementary insights into continual adaptation and serve as broader context for studying more structured forms of real-world non-stationarity.

3. Preliminaries

3.1. Stage-Aware Class-Incremental Learning

In standard Class-Incremental Learning (CIL), a model is trained on a sequence of tasks $\mathcal{T} = \{T_1, T_2, \dots, T_{N_{\text{task}}}\}$. Each task T_t provides a dataset $D_t = \{(x_i, y_i)\}_{i=1}^{n_t}$, where x_i is an input sample and $y_i \in \mathcal{C}_t$ is its class label. The class sets are disjoint across tasks, $\mathcal{C}_t \cap \mathcal{C}_{t'} = \emptyset$ for $t \neq t'$, and we denote the cumulative label space up to task t as $\mathcal{C}_{1:t} = \bigcup_{j=1}^t \mathcal{C}_j$. During training on T_t , the model only has access to D_t . The goal of CIL is to achieve high performance on all classes seen so far, i.e., on $\mathcal{C}_{1:t}$ after each task, while mitigating catastrophic forgetting of earlier classes.

Stage-Aware Class-Incremental Learning (Stage-CIL) extends this paradigm by introducing an *ordered morphological stage* for each sample. Each training example is a triplet (x_i, y_i, s_i) , where x_i is the input, $y_i \in \mathcal{C}_t$ is the class label, and $s_i \in \mathcal{S} = \{0, 1, \dots, M-1\}$ is a discrete stage index from a fixed set of M stages. The prediction target at test time remains the class label y_i , while the stage index s_i provides structured side information about where an instance lies along its class-specific evolution.

For a given task T_t , we can decompose its dataset into stage-specific subsets

$$D_t^{(s)} = \{(x_i, y_i, s_i) \in D_t \mid s_i = s\}, \quad D_t = \bigcup_{s=0}^{M-1} D_t^{(s)}.$$

The training stream is organized such that, for any fixed class $c \in \mathcal{C} = \bigcup_t \mathcal{C}_t$, its stages are encountered in non-decreasing order: data from stage s of class c never appears after we have already seen stage $s' > s$ of the same class.¹ This induces a sequence of *task–stage pairs*, and we index the corresponding learning steps by $b = 1, \dots, B$.

Compared to conventional CIL, the objective of Stage-CIL is strictly more demanding. After completing training on all task–stage pairs, the model is evaluated on *all* combinations of previously seen classes and stages. In particular, it must (i) distinguish between different classes (*inter-class discrimination*) and simultaneously (ii) maintain a coherent identity for each class across its stages (*intra-class coherence*). This second requirement introduces the novel challenge of **intra-class forgetting**. This phenomenon does not arise in

¹In our benchmark (Stage-Bench), we adopt $M = 2$ and focus on the transition from an initial stage ($s = 0$) to an evolved stage ($s = 1$).

standard CIL, as its protocols implicitly assume that classes are morphologically static.

3.2. Evaluation Protocol and Metrics

We build on standard CIL evaluation protocols (Rebuffi et al., 2017; Wang et al., 2022c), and extend them to the Stage-CIL setting. A configuration is denoted as $(B-m, \text{Inc}-n) \times S^M$, where an initial *base* session introduces m classes, each incremental session introduces n new classes, and each class appears across M temporally ordered stages. The overall training stream can be viewed as B ordered learning steps (task–stage pairs). After each step $b \in \{1, \dots, B\}$, we measure the Top-1 accuracy \mathcal{A}_b on all classes and stages observed up to that point. The average incremental accuracy is then defined as $\bar{\mathcal{A}} = \frac{1}{B} \sum_{b=1}^B \mathcal{A}_b$. To analyze forgetting more finely, we adopt and extend class-wise metrics. Let $N_{\text{cls}} = |\mathcal{C}|$ denote the total number of classes in the benchmark, and let $A_i(b)$ be the accuracy for class i at step b (aggregated over all its stages that have been introduced by step b).

Inter-class forgetting (Inter-F). Following (Chaudhry et al., 2018), we define Inter-F as the average drop from the best-achieved accuracy of each class to its final accuracy:

$$F_{\text{inter}} = \frac{1}{N_{\text{cls}}} \sum_{i=1}^{N_{\text{cls}}} \left(\max_{1 \leq b \leq B} A_i(b) - A_i(B) \right). \quad (1)$$

A higher F_{inter} indicates more severe forgetting of previously learned classes in the conventional CIL sense.

Intra-class forgetting (Intra-F). To quantify the model’s ability to preserve identity across a class’s own morphological stages, we introduce the Intra-F metric. In its general form, it measures the performance degradation between the first-seen stage and the last-seen stage for each class. Let $A_{i,s}$ denote the accuracy for class i on its stage- s test set, evaluated at the final learning step B . The intra-class forgetting is defined as the normalized accuracy drop from the initial stage ($s = 0$) to the final stage ($s = M-1$):

$$F_{\text{intra}} = \frac{1}{N_{\text{cls}}} \sum_{i=1}^{N_{\text{cls}}} \frac{A_{i,0} - A_{i,M-1}}{\max(\epsilon, A_{i,0})}, \quad \epsilon = 10^{-6}. \quad (2)$$

A larger F_{intra} indicates a greater loss of stage-wise coherence for a class across its full evolution. **For our two-stage benchmark, Stage-Bench ($M = 2$), this becomes:**

$$F_{\text{intra}} = \frac{1}{N_{\text{cls}}} \sum_{i=1}^{N_{\text{cls}}} \frac{A_{i,\text{Stage-0}} - A_{i,\text{Stage-1}}}{\max(\epsilon, A_{i,\text{Stage-0}})}. \quad (3)$$

Unlike Inter-F, which captures forgetting across classes, Intra-F isolates degradation *within* each class by measuring the average relative drop between stages, making it a metric uniquely suited to the Stage-CIL setting and a crucial diagnostic for evolution-specific forgetting.

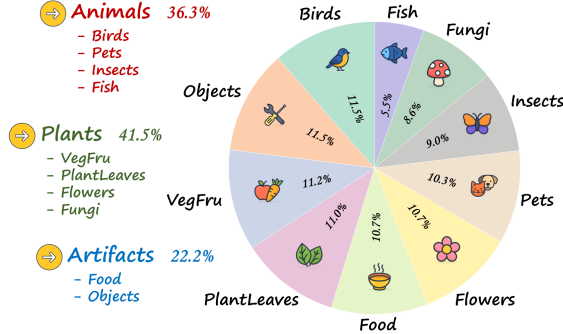


Figure 2. Statistical summary of **Stage-Bench**. It spans 10 diverse domains, each with 20 classes and two ordered stages (Stage-0 and Stage-1), yielding 400 morphological stages in total.

3.3. Benchmark

To concretely instantiate the Stage-CIL paradigm and its metrics, we construct and release **Stage-Bench**. The design of this benchmark follows a simple scientific principle: first isolate and rigorously measure the most challenging form of intra-class evolution before moving to finer-grained, multi-stage settings. We observe that, for many entities, the most drastic morphological shift occurs between an initial and a final phase of their lifecycle. Accordingly, Stage-Bench models evolution as a two-stage transition ($M = 2$), focusing on the passage from an initial morphology (Stage-0) to an evolved morphology (Stage-1). This "maximal gap" design yields a clear and demanding stress test for intra-class coherence, making it possible to attribute performance changes directly to the ability to handle evolution.

Stage-Bench spans ten diverse domains (*Fish*, *Flowers* (Nilsback et al., 2008), *Food* (Bossard et al., 2014), *VegFru* (Hou et al., 2017), *Fungi*, *Insects*, *Birds* (Van Horn et al., 2015), *Pets* (Parkhi et al., 2012), *PlantLeaves*, *Objects* (Bergmann et al., 2019)). Each domain provides 20 classes, and each class is annotated with two ordered morphological stages: Stage-0 (initial) and Stage-1 (evolved). While any discrete annotation is an abstraction, our stages are aligned with semantically meaningful, real-world milestones rather than synthetic augmentations, providing precisely the structured supervision that conventional CIL datasets lack.

In total, Stage-Bench contains 18,895 images, with a roughly 1 : 1 balance between Stage-0 and Stage-1, as summarized in Figure 2. Images are sourced from public benchmarks and the web, followed by rigorous cleaning and expert verification to ensure both class and stage correctness. We release official train/validation/test splits, mapping files, and data loaders to facilitate reproducible evaluation under the $(B - m, Inc - n) \times S^2$ protocol. Further details on data collection, licensing, and ethical considerations are provided in the supplementary material.

4. Methodology

Facing the challenge of Stage-CIL, STAGE employs a predict-then-classify framework tailored for the ordered structure of Stage-CIL. It decouples transformation dynamics from class identity maintenance via a bespoke Evolution-aware Memory Pool. Rather than a passive buffer, this pool acts as an active inference engine: it distills a stable prototype from initial observations and iteratively predicts evolved representations for subsequent morphologies prior to classification. Fig.3 and Alg.1 detail the workflow and training procedure.

4.1. Predictive Evolution Framework

Anchor Distillation (Phase 0). When a class is first observed (at stage s_0), STAGE focuses on distilling a stable *anchor* prototype $p_c^{s_0}$ that will serve as the identity reference for all subsequent evolution. Following common practice in PTM-based CIL (Zhou et al., 2025b), we freeze the vision-language backbone ($g_{\text{img}}, g_{\text{text}}$) and introduce learnable, task-specific projection layers. These projections are trained exclusively on the first-seen samples $D_t^{s_0}$. After training, the final anchor $p_c^{s_0}$ is constructed by computing a class-mean visual prototype $\mathbf{v}_c^{s_0}$ and then fusing it with its textual representation \mathbf{t}_c via cross-modal attention:

$$\mathbf{v}_c^{s_0} = \frac{1}{|D_c^{s_0}|} \sum_{x_i \in D_c^{s_0}} g_{\text{img}}(x_i), \quad (4)$$

$$p_c^{s_0} = W_q^t \mathbf{v}_c^{s_0} + \text{Attn}(W_q^t \mathbf{v}_c^{s_0}, W_k^t \mathbf{t}_c, W_v^t \mathbf{t}_c), \quad (5)$$

where $D_c^{s_0}$ is the set of initial-stage samples for class c . This anchor serves as the stable starting point for all subsequent predictions.

Predictive Evolution via Memory Pool (Phase 1). For any subsequent stage $s + 1$, STAGE reuses the anchor $p_c^{s_0}$ to forecast the next-stage sample feature $\hat{\mathbf{x}}_i^{s+1}$. This avoids re-tuning the classifier on mixed-stage features, which could corrupt the stable anchor. The prediction is driven by the **Evolution-aware Memory Pool**, a fixed-size, learnable memory $\mathcal{P} = \{u_1, \dots, u_K\}$ of basis transformation patterns (e.g., "color darkens").

Anchored on $p_c^{s_0}$, the predictor selects the top- k most relevant patterns from \mathcal{P} via cosine similarity. These patterns, indexed by the active set $I_{c,i}$, form a transformation context $\mathbf{c}_{c,i}$ through an attention mechanism. This context is then used to predict the evolved feature in a residual manner with an evolution network $E(\cdot)$:

$$\mathbf{c}_{c,i} = \text{Attn}(p_c^{s_0}, \{u_j\}_{j \in I_{c,i}}), \quad (6)$$

$$\hat{\mathbf{x}}_i^{s+1} = p_c^{s_0} + E(p_c^{s_0} + \mathbf{c}_{c,i}). \quad (7)$$

This formulation is a key aspect of our method. Although the basis patterns $\{u_j\}$ are linearly combined, the input-

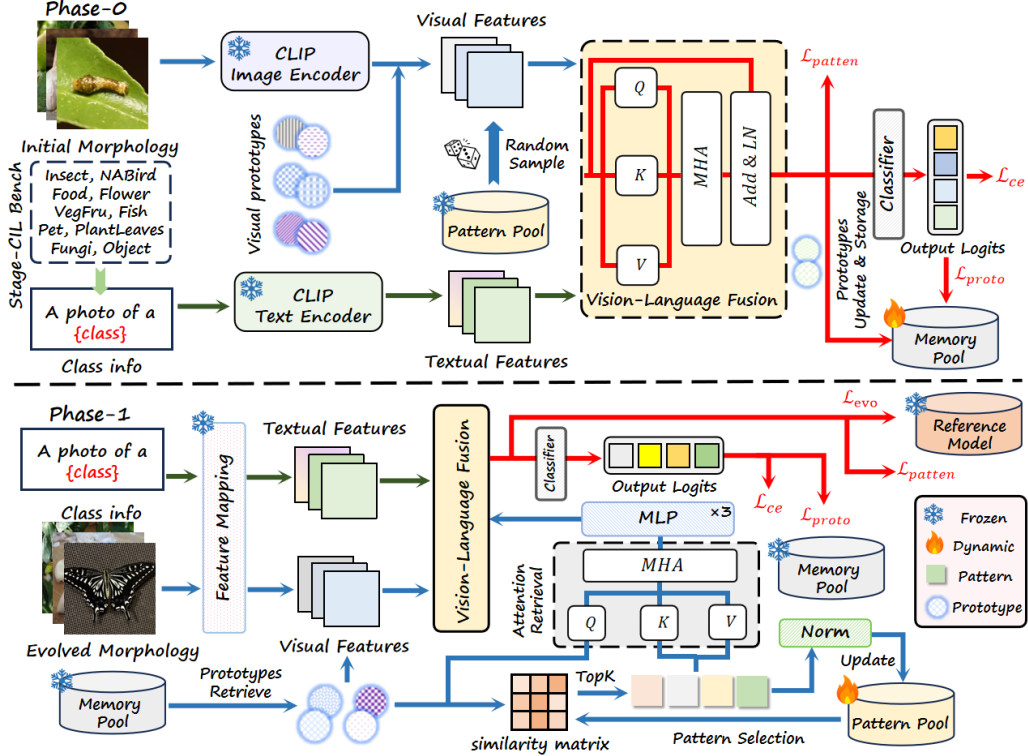


Figure 3. Illustration of STAGE. **Top:** the model learns a visual prototype for each new class from initial-morphology images, while text prompts provide class semantics. **Bottom:** the stored prototype queries the pattern pool, attends to the top-k patterns, and predicts the evolved representation of the Stage 1 images and online pattern updates.

dependent top- k gating and the nonlinear head $E(\cdot)$ make the overall operator a piecewise-smooth, non-linear function, akin to a sparse Mixture-of-Experts model. This provides the flexibility to approximate complex, non-linear transformations.

Online Pattern Adaptation. The memory pool is updated online to refine its transformation patterns. This process is supervised at the prototype level. Given the paired prototypes for an observed transition (p_c^s, p_c^{s+1}) , the active patterns are updated via a competitive, stochastic moving average rule as follows:

$$u_j \leftarrow (1 - \eta) u_j + \eta w_{i,j} (p_c^{s+1} - p_c^s), \quad \forall j \in I_{c,i}, \quad (8)$$

where $w_{i,j}$ is the attention weight. This update rule acts as a temporal low-pass filter, allowing the pool to slowly distill persistent and general transformation signals while averaging out sample-specific noise. It effectively separates the learning timescales: the memory pool learns slow, general dynamics, while the network $E(\cdot)$ adapts more quickly to task-specific features via gradient descent. This dual-timescale learning is crucial for stability in a continual learning setting.

4.2. Training Objectives

The training objective is designed for both robust knowledge retention and accurate transformation modeling. During the initial stage (**Phase 0**), the loss focuses on classification and stability:

$$\mathcal{L}_{\text{Phase0}} = \mathcal{L}_{\text{ce}} + \gamma \mathcal{L}_{\text{proto}} + \delta \mathcal{L}_{\text{pattern}}. \quad (9)$$

Here, \mathcal{L}_{ce} is the standard cross-entropy loss, $\mathcal{L}_{\text{proto}}$ is a rehearsal loss on prototypes from previous tasks, and $\mathcal{L}_{\text{pattern}}$ regularizes the evolution network. The pattern rehearsal loss encourages identity-like behavior when no genuine transformation is present, and is defined as:

$$\mathcal{L}_{\text{pattern}} = \mathbb{E}_{u_j \sim \mathcal{P}} \|E(p_c^{s_0} + \text{Attn}(p_c^{s_0}, \{u_j\}))\|_2^2. \quad (10)$$

In subsequent stages (**Phase 1**), we introduce a composite evolution loss, \mathcal{L}_{evo} , to supervise the prediction of individual sample features:

$$\begin{aligned} \mathcal{L}_{\text{evo}} = & \|\hat{\mathbf{x}}_i^{s+1} - \mathbf{x}_i^{s+1}\|_2^2 \\ & + \lambda_{\text{cos}} \left(1 - \cos (\hat{\mathbf{x}}_i^{s+1} - \mathbf{p}_c^{s_0}, \mathbf{x}_i^{s+1} - \mathbf{p}_c^{s_0}) \right), \end{aligned} \quad (11)$$

where \mathbf{x}_i^{s+1} is the ground-truth feature and $\mathbf{p}_c^{s_0}$ is the class anchor. The total loss for Phase 1 integrates this evolution

Algorithm 1 STAGE Training Procedure

```

1: Input: Task sequence  $T = \{T_1, \dots, T_N\}$ ; For each  $T_t$ :  $D_t^0, D_t^1$ ; Pattern pool  $\mathcal{P}$ ; Evolution net  $E$ .
2: for each task  $T_t \in T$  do
3:   Phase 0: Train on  $D_t^0$ 
4:     Compute visual prototypes via Eq. (4)
5:     Fuse with textual prompts via Eq. (5)
6:     Store fused prototypes  $p_c^{s_0}$  in memory buffer
7:   Phase 1:
8:     for each  $(x, y) \in D_t^1$  do
9:       Retrieve anchor  $p_c^{s_0}$  from memory buffer
10:      Select top- $k$  patterns by cosine similarity
11:      Predict  $\hat{x}_i^{s+1}$  via Eq. (7)
12:      Compute evolution loss via Eq. (11)
13:      Compute rehearsal losses via Eq. (10)
14:      Update model via Eq. (12)
15:      Update top- $k$  patterns in  $\mathcal{P}$  via Eq. (8)
16:     end for
17:   end for

```

loss with the same rehearsal terms:

$$\mathcal{L}_{\text{Phase1}} = \mathcal{L}_{\text{ce}} + \alpha \mathcal{L}_{\text{evo}} + \gamma \mathcal{L}_{\text{proto}} + \delta \mathcal{L}_{\text{pattern}}. \quad (12)$$

This dual-objective training, combined with the reusable predictive operator, ensures the framework’s applicability to multi-stage evolution without architectural changes or memory growth.

5. Experiment

In this section, we validate the Stage-CIL paradigm and the Stage-Bench benchmark. We first establish the performance of various state-of-the-art (SOTA) CIL and DIL methods on this new benchmark, revealing the unique challenges posed by intra-class evolution. We then show STAGE effectively addresses these challenges. Finally, a comprehensive ablation study and visual analysis are provided to dissect the key components of our approach.

5.1. Implementation Details

Dataset protocol. For all experiments, we follow the protocol of the Stage-Bench described in metrics, using the (B-0, Inc-10) \times S² setting our dataset (400 morphological stages, 200 classes \times 2 stages), which unfolds over 20 incremental steps and a total of 40 tasks. All experiments use a fixed random seed of 1993 for class order shuffling, and all methods are evaluated on the identical sequence of tasks and data splits for fair comparison, following (Zhou et al., 2025a). Additionally, to test the multi-stage generalization of our framework, we restructured the Object domain into a three-stage evolution task, evaluated under the same protocol.

Training Details. We use Pytorch (Paszke et al., 2019)

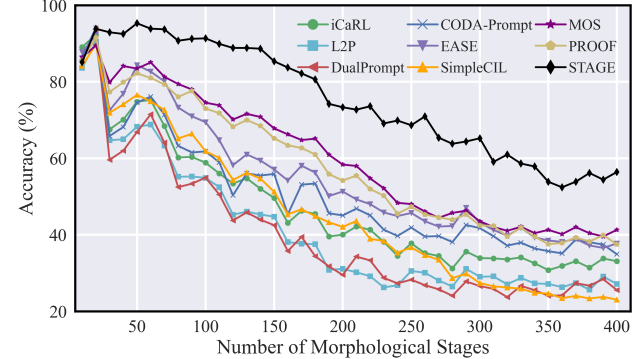


Figure 4. Incremental performance of different methods. We report the performance gap after the last incremental stage of STAGE and the runner-up method at the end of the line. All methods are based on the same backbone/weight.

and PILOT (Sun et al., 2025a) to implement all models on two NVIDIA TITAN X GPUs. We use the *same* network backbone, *i.e.*, CLIP with ViT-B/16 (OpenCLIP LAION-400M) (Ilharco et al., 2021) for all compared methods for *fair comparison*. We set the batch size to 16 and train for 5 epochs using SGD with momentum for optimization. The learning rate starts 0.001 and decays with cosine annealing. In practice, we interleave classification and evolution updates in Phase-1, rehearse a small, uniformly random subset of the memory pool per step, and use a small EMA rate for stable adaptation.

Comparison methods. We evaluate STAGE against a comprehensive suite of state-of-the-art incremental learning methods. We select prominent Pre-Trained Model-based approaches, including prompt-tuning methods like L2P (Wang et al., 2022c), DualPrompt (Wang et al., 2022b) and CODA-Prompt (Smith et al., 2023), as well as other superior methods such as EASE (Zhou et al., 2024b), SimpleCIL (Zhou et al., 2025a), MOS (Sun et al., 2025b) and PROOF (Zhou et al., 2025b). Furthermore, to represent the perspective of DIL, which views stage evolution as a sequence of domain shifts, we include leading methods such as S-Prompts (Wang et al., 2022a) and DCE (Li et al., 2025). In addition, we compare our model with a classic rehearsal-based method, iCaRL (Rebuffi et al., 2017), which we adapt for a PTM-based framework. To ensure a fair and rigorous comparison, all methods are implemented using the same PTM backbone and experimental protocol.

5.2. Benchmark Comparison

In this section, we conduct a comprehensive evaluation of STAGE against other SOTA methods on Stage-Bench. The complete results, including final accuracy and average incremental accuracy, are detailed in Table 1. On the primary two-stage benchmark, a clear performance hierarchy

Table 1. Average, last performance, inter- and intra-forgetting comparison on Stage-CIL using CLIP with ViT-B/16 LAION-400M as the backbone. The left part shows results on Stage-Bench(2-stage), and the right part shows results on the restructured Object domain(3-stage). The best performance is shown in **bold**. All methods are initialized with the same pre-trained CLIP for a fair comparison.

Method	Stage-Bench (B-0 Inc-10) $\times S^2$						Object (B-0 Inc-10) $\times S^3$		
	$\bar{\mathcal{A}}$	\mathcal{A}_B	$\mathcal{A}_{B,0}$	$\mathcal{A}_{B,1}$	Inter-F	Intra-F	$\bar{\mathcal{A}}$	\mathcal{A}_B	Intra-F
iCaRL (CVPR 2017)	47.26	33.12	25.41	32.89	24.31	36.42	94.67	95.83	1.52
L2P (CVPR 2022)	41.05	27.16	21.96	32.43	26.77	51.08	92.84	93.42	2.67
DualPrompt (ECCV 2022)	40.08	25.56	19.63	31.59	28.53	47.33	92.26	93.76	2.92
CODA-Prompt (CVPR 2023)	50.77	34.93	30.70	39.24	24.04	38.19	95.42	96.38	1.35
EASE (CVPR 2024)	50.57	37.75	33.94	41.62	21.85	27.05	95.18	96.52	1.28
SimpleCIL (IJCV 2024)	45.74	23.07	18.11	28.13	26.18	58.61	93.91	94.25	2.18
MOS (AAAI 2025)	59.74	41.31	37.95	44.73	19.86	24.44	97.25	97.42	0.68
PROOF (TPAMI 2025)	57.77	37.52	33.09	42.03	20.39	29.37	96.21	97.15	1.07
S-Prompts (NIPS 2022)	44.32	29.18	22.47	35.89	25.64	42.76	93.15	94.02	2.35
DCE (ICML 2025)	53.86	38.94	34.12	43.76	22.15	22.58	95.87	96.73	0.86
STAGE	75.11	56.44	55.68	57.21	16.92	7.48	98.44	98.61	0.31

emerges: existing methods tailored for inter-class knowledge isolation struggle to cope with the drastic morphological shifts in Stage-CIL, reflected by their high Inter-F and even higher Intra-F values. In contrast, STAGE consistently achieves the best performance across all primary continual learning metrics. As visualized in Figure 4, STAGE establishes a substantial lead from the early tasks and the advantage widens as more classes and stages are introduced, culminating in a gap of over 15% in final accuracy by the final tasks. This highlights our model’s superior scalability and robustness in long-sequence evolutionary scenarios. Crucially, on the restructured three-stage Object domain, STAGE maintains a significant lead, achieving a remarkably low Intra-F of 0.31%. This validates the generalizability of our stage-agnostic predictive mechanisms.

5.3. Ablation Study

To dissect the contributions of STAGE’s key components, we conduct an incremental ablation study, with results shown in Figure 5. The ”Baseline” model, lacking any evolution-aware mechanisms, exhibits poor performance, confirming the difficulty of the Stage-CIL task. The most significant performance gain comes from introducing the ”w/ Evolution-aware Memory Pool”. This highlights that our core predict-then-classify paradigm is the primary driver of success, effectively mitigating the large feature drift between stages. Adding ”w/ Prototype Rehearsal” provides a further, stable improvement, underscoring the necessity of combating traditional inter-class forgetting even while addressing the new intra-class challenge. Finally, ”w/ Pattern Rehearsal” offers an additional small boost by regularizing the memory pool and preventing pattern collapse. This analysis confirms that while the predictive memory pool is the core innovation, all components work in synergy to achieve the final robust performance.

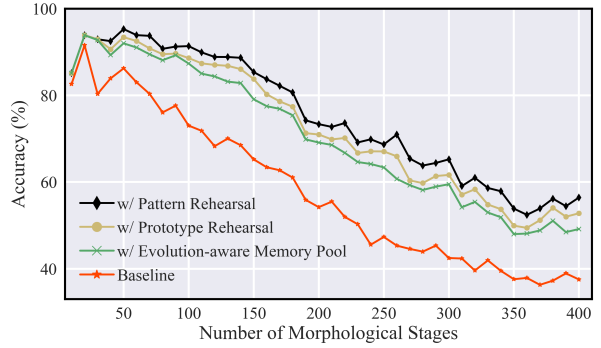


Figure 5. Ablation study of different components in STAGE. We find each component within STAGE enhances the performance.

We further investigate the sensitivity to pattern pool size and top- k selection, with results in Table 2. Our analysis indicates that a pool size of 50 with $k = 5$ provides an optimal balance between performance and efficiency. Smaller pools (Pattern 10) show degraded performance due to insufficient expressive capacity, while larger pools (Pattern 100) offer diminishing returns for the increased computational cost. Regarding top- k selection, $k = 5$ outperforms both alternatives. A single pattern ($k = 1$) is too restrictive for complex transformations, leading to a sharp rise in Intra-F. Conversely, a larger selection ($k = 10$) appears to introduce noise from less relevant patterns, degrading overall accuracy. These findings validate our chosen configuration.

5.4. Visualization

Figure 6 illustrates the performance comparison between STAGE and baseline methods across incremental tasks, with accuracy metrics reported for both Stage 0 and Stage 1 data. The shaded region between the two curves represents the intra-class forgetting gap; a narrower gap indicates better

Table 2. Parameter analysis of STAGE on Stage-Bench. We report average incremental accuracy $\bar{\mathcal{A}}$, final accuracy \mathcal{A}_B , inter-class forgetting (Inter-F), and intra-class forgetting (Intra-F) under different pattern pool sizes and top- k selections.

Stage-Bench (B-0 Inc-10) $\times S^2$				
Configuration	$\bar{\mathcal{A}}$	\mathcal{A}_B	Inter-F	Intra-F
Pattern Pool Size (Top-5)				
Pattern 10	71.15	47.60	19.48	15.73
Pattern 50	75.11	56.44	16.92	7.48
Pattern 100	76.12	57.38	16.80	6.83
Top-k Selection (Pool Size 50)				
Top-1	71.13	47.29	19.84	18.05
Top-5	75.11	56.44	16.92	7.48
Top-10	73.20	52.31	17.83	9.16

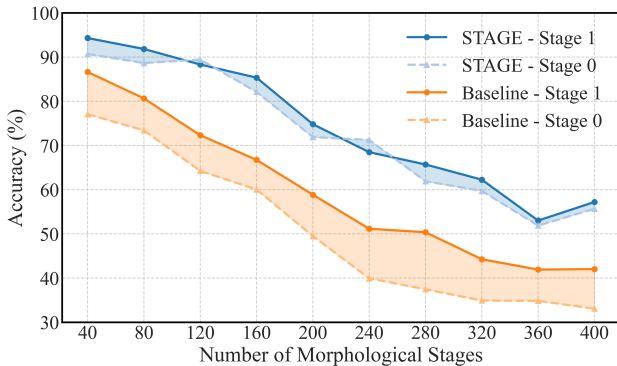


Figure 6. Accuracy gap between Stage-0 and Stage-1 test samples for STAGE and the Baseline. The gap is measured after the completion of each domain on the Stage-Bench.

preservation of knowledge across morphological evolution. STAGE achieves significantly higher accuracy in both stages while maintaining a consistently smaller gap, effectively preserving coherent class identities throughout the evolutionary trajectory. This validates that our evolution-aware Memory Pool successfully mitigates intra-class forgetting by learning structured, transferable transformations. To validate the interpretability and effectiveness of our framework, we employ Grad-CAM (Selvaraju et al., 2017) for comparative visualization. As illustrated in Figure 7, STAGE consistently focuses on semantically meaningful regions critical to morphological evolution, such as specific body parts of insects undergoing transformation or newly emerging features in birds. In contrast, PROOF tends to concentrate on the overall object, neglecting dynamic regions associated with developmental changes. This demonstrates that STAGE adaptively attends to key evolutionary features rather than overfitting to global object identity, capturing essential cues of morphological transformation.

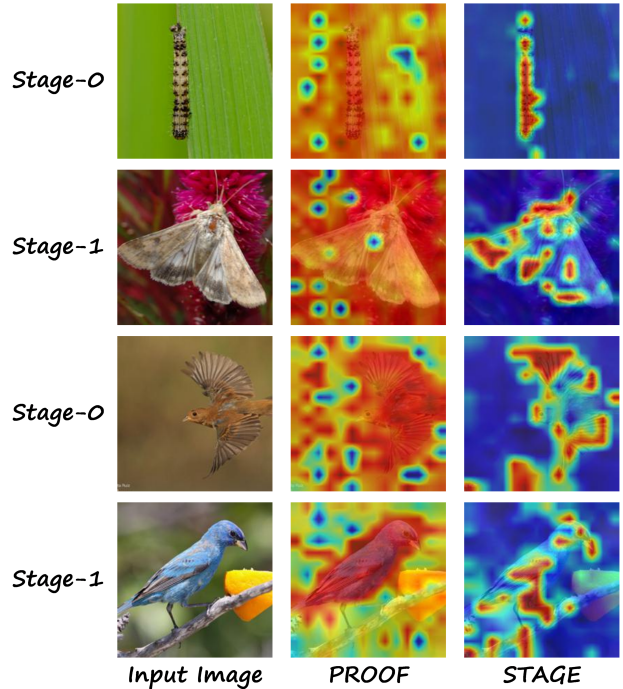


Figure 7. Grad-CAM comparison between different stage images by PROOF and STAGE. It shows that STAGE focus on key evolutionary features of the entity.

6. Conclusion

In this paper, we introduced Stage-Aware Class-Incremental Learning (Stage-CIL), a new paradigm for learning classes that undergo significant morphological evolution. To support systematic research on this problem, we presented **Stage-Bench**, the first 10-domain benchmark and protocol to explicitly measure both inter- and intra-class forgetting. We then proposed STAGE, a stage-agnostic, *predict-then-classify* framework that serves as a baseline for this new task. By decoupling stable identity from transformation dynamics, STAGE substantially outperforms existing CIL and DIL methods, demonstrating that explicit evolution modeling is a practical and effective approach. We note that the success of this paradigm relies on reliable stage supervision and well-structured pre-trained representations. Furthermore, while the predictive step is efficient, the online adaptation of the memory pool introduces a modest computational overhead compared to non-adaptive methods. Exploring robustness to practical challenges such as noisy annotations and violations of the assumed temporal ordering are therefore directions for future researches and extensions.

References

Bergmann, P., Fauser, M., Sattlegger, D., and Steger, C. MVTec AD — a comprehensive real-world dataset for unsupervised anomaly detection. In *Proceedings of the*

IEEE/CVF Conference on Computer Vision and Pattern Recognition, pp. 9592–9600, 2019.

Bossard, L. et al. Food-101 – mining discriminative components with random forests. In *European Conference on Computer Vision*, pp. 446–461. Springer, 2014.

Chaudhry, A., Dokania, P. K., Ajanthan, T., and Torr, P. H. S. Riemannian walk for incremental learning: Understanding forgetting and intransigence. In *Proceedings of the European Conference on Computer Vision (ECCV)*, pp. 532–547. Springer, 2018.

Choi, S., Kim, W., Kim, S., In, Y., Kim, S., and Park, C. Dslr: diversity enhancement and structure learning for rehearsal-based graph continual learning. In *Proceedings of the ACM Web Conference 2024*, pp. 733–744, 2024.

De Lange, M., Aljundi, R., Masana, M., Parisot, S., Jia, X., Leonardis, A., Slabaugh, G., and Tuytelaars, T. A continual learning survey: Defying forgetting in classification tasks. *IEEE transactions on pattern analysis and machine intelligence*, 44(7):3366–3385, 2021.

Feng, Y., Tian, Z., Zhu, Y., Han, Z., Luo, H., Zhang, G., and Song, M. Cp-prompt: Composition-based cross-modal prompting for domain-incremental continual learning. In *Proceedings of the 32nd ACM International Conference on Multimedia*, pp. 2729–2738, 2024.

French, R. M. Catastrophic forgetting in connectionist networks. *Trends in cognitive sciences*, 3(4):128–135, 1999.

Hou, S., Feng, Y., and Wang, Z. Vegfru: A domain-specific dataset for fine-grained visual categorization. In *Proceedings of the IEEE International Conference on Computer Vision (ICCV)*, Oct 2017.

Ilharco, G., Wortsman, M., Wightman, R., Gordon, C., Carlini, N., Taori, R., Dave, A., Shankar, V., Namkoong, H., Miller, J., Hajishirzi, H., Farhadi, A., and Schmidt, L. OpenCLIP: Open-source implementation of clip. <https://doi.org/10.5281/zenodo.5143773>, 2021.

Jiang, S., Zhang, D., Cheng, F., Lu, X., and Liu, Q. Dupt: Rehearsal-based continual learning with dual prompts. *Neural Networks*, 187:107306, 2025.

Jung, C., Kim, S., Yoon, S., and Kim, H. Dynamic adaptive prompts for continual learning. In *Proceedings of the IEEE/CVF International Conference on Computer Vision*, pp. 14145–14155, 2023.

Kirkpatrick, J., Pascanu, R., Rabinowitz, N., et al. Overcoming catastrophic forgetting in neural networks. In *Proceedings of the National Academy of Sciences*, volume 114, pp. 3521–3526. National Academy of Sciences, 2017.

Langley, P. Crafting papers on machine learning. In Langley, P. (ed.), *Proceedings of the 17th International Conference on Machine Learning (ICML 2000)*, pp. 1207–1216, Stanford, CA, 2000. Morgan Kaufmann.

Li, L., Zhou, D.-W., Ye, H.-J., and Zhan, D.-C. Addressing imbalanced domain-incremental learning through dual-balance collaborative experts. In *Proceedings of the International Conference on Machine Learning*, 2025.

Li, Z. and Hoiem, D. Learning without forgetting. *IEEE Transactions on Pattern Analysis and Machine Intelligence*, 40(12):2935–2947, 2018. doi: 10.1109/TPAMI.2017.2773081.

McCloskey, M. et al. Catastrophic interference in connectionist networks: The sequential learning problem. In *Psychology of learning and motivation*, volume 24, pp. 109–165. Elsevier, 1989.

McDonnell, M. D., Gong, D., Parvaneh, A., Abbasnejad, E., and van den Hengel, A. Rancpac: Random projections and pre-trained models for continual learning. In *Advances in Neural Information Processing Systems*, volume 36, 2023.

Nilsback, M.-E. et al. Automated flower classification over a large number of classes. In *2008 Sixth Indian conference on computer vision, graphics & image processing*, pp. 722–729. IEEE, 2008.

Parkhi, O. M., Vedaldi, A., Zisserman, A., and Jawahar, C. V. Cats and dogs. In *Proceedings of the IEEE Conference on Computer Vision and Pattern Recognition*, pp. 3498–3505, 2012.

Paszke, A., Gross, S., Massa, F., Lerer, A., Bradbury, J., Chanan, G., Killeen, T., Lin, Z., Gimelshein, N., Antiga, L., Desmaison, A., Köpf, A., Yang, E. Z., DeVito, Z., Raison, M., Tejani, A., Chilamkurthy, S., Steiner, B., Fang, L., Bai, J., and Chintala, S. Pytorch: An imperative style, high-performance deep learning library. In *Advances in Neural Information Processing Systems (NeurIPS)*, pp. 8024–8035, 2019.

Rebuffi, S.-A., Kolesnikov, A., Sperl, G., and Lampert, C. H. icarl: Incremental classifier and representation learning. In *Proceedings of the IEEE conference on Computer Vision and Pattern Recognition*, pp. 2001–2010, 2017.

Rusu, A. A., Rabinowitz, N. C., Desjardins, G., Soyer, H., Kirkpatrick, J., Kavukcuoglu, K., and Pascanu, R. Progressive neural networks for lifelong learning. In *Proceedings of the 31st International Conference on Neural Information Processing Systems*, volume 30, 2017.

Selvaraju, R. R., Cogswell, M., Das, A., Vedantam, R., Parikh, D., and Batra, D. Grad-cam: Visual explanations from deep networks via gradient-based localization. In *Proceedings of the IEEE international conference on computer vision*, pp. 618–626, 2017.

Shaheen, K., Hanif, M. A., Hasan, O., and Shafique, M. Continual learning for real-world autonomous systems: Algorithms, challenges and frameworks. *Journal of Intelligent & Robotic Systems*, 105(1):9, 2022.

Smith, J. S., Karlinsky, L., Gutta, V., Cascante-Bonilla, P., Kim, D., Arbelle, A., Panda, R., Feris, R., and Kira, Z. Coda-prompt: Continual decomposed attention-based prompting for rehearsal-free continual learning. In *Proceedings of the IEEE/CVF conference on computer vision and pattern recognition*, pp. 11909–11919, 2023.

Sun, H.-L., Zhou, D.-W., Ye, H.-J., and Zhan, D.-C. Pilot: A pre-trained model-based continual learning toolbox. *Science China Information Sciences*, 68(4):147101, 2025a. doi: 10.1007/s11432-024-4276-4.

Sun, H.-L., Zhou, D.-W., Zhao, H., Gan, L., Zhan, D.-C., and Ye, H.-J. Mos: Model surgery for pre-trained model-based class-incremental learning. In *Proceedings of the AAAI Conference on Artificial Intelligence*, volume 39, pp. 20699–20707, 2025b.

van de Ven, G. M. and Tolias, A. S. Three types of incremental learning. *Nature Machine Intelligence*, 4:8–10, 2022.

Van Horn, G., Branson, S., Farrell, R., Haber, S., Barry, J., Ipeirotis, P., Perona, P., and Belongie, S. Building a bird recognition app and large scale dataset with citizen scientists: The fine print in fine-grained dataset collection. In *Proceedings of the IEEE conference on computer vision and pattern recognition*, pp. 595–604, 2015.

Wang, L., Zhang, X., Su, H., and Zhu, J. A comprehensive survey of continual learning: Theory, method and application. *IEEE transactions on pattern analysis and machine intelligence*, 46(8):5362–5383, 2024.

Wang, Y., Huang, Z., and Hong, X. S-Prompts learning with pre-trained transformers: An occam’s razor for domain incremental learning. In *Advances in Neural Information Processing Systems*, volume 35, pp. 5682–5695, 2022a.

Wang, Z., Zhang, Z., Ebrahimi, S., Sun, R., Zhang, H., Lee, C.-Y., Ren, X., Su, G., Perot, V., Dy, J., et al. Dualprompt: Complementary prompting for rehearsal-free continual learning. In *European conference on computer vision*, pp. 631–648. Springer, 2022b.

Wang, Z., Zhang, Z., Lee, C.-Y., Zhang, H., Sun, R., Ren, X., Su, G., Perot, V., Dy, J., and Pfister, T. Learning to prompt for continual learning. In *Proceedings of the IEEE/CVF conference on computer vision and pattern recognition*, pp. 139–149, 2022c.

Zhou, D.-W., Sun, H.-L., Ning, J., Ye, H.-J., and Zhan, D.-C. Continual learning with pre-trained models: A survey. *arXiv preprint arXiv:2401.16386*, 2024a.

Zhou, D.-W., Sun, H.-L., Ye, H.-J., and Zhan, D.-C. Expandable subspace ensemble for pre-trained model-based class-incremental learning. In *Proceedings of the IEEE/CVF Conference on Computer Vision and Pattern Recognition*, pp. 23554–23564, 2024b.

Zhou, D.-W., Cai, Z.-W., Ye, H.-J., Zhan, D.-C., and Liu, Z. Revisiting class-incremental learning with pre-trained models: Generalizability and adaptivity are all you need. *International Journal of Computer Vision*, 133(3):1012–1032, 2025a.

Zhou, D.-W., Zhang, Y., Wang, Y., Ning, J., Ye, H.-J., Zhan, D.-C., and Liu, Z. Learning without forgetting for vision-language models. *IEEE Transactions on Pattern Analysis and Machine Intelligence*, 47(6):4489–4504, 2025b.

Zhou, X., Liu, Z., Tian, Y., Chen, Y., Hu, X., Hu, C., and Wang, Z. Prompting makes pre-trained models strong class incremental learners. *arXiv preprint arXiv:2312.02469*, 2024c.

A. Appendix

In this supplementary material, we provide additional details and analyses that complement the main paper on Stage-CIL. The content is organized as follows:

- **Details of Stage-Bench (Section 1)** gives a detailed description of the Stage-Bench dataset, including domain composition, data sources, stage annotation procedure, and licensing/ethical considerations, together with illustrative examples of Stage-0/Stage-1 pairs.
- **Introduction about Compared Methods (Section 2)** summarizes the PTM-based CIL and DIL baselines used in our experiments and explains, for each method, its core limitations when instantiated under the Stage-CIL protocol.
- **Additional Analysis of STAGE (Section 3)** studies the internal behaviour and cost of our framework, including an analysis of the three-phase dynamics of the shared pattern pool and a computational/memory complexity discussion on top of the frozen CLIP backbone.
- **Additional Experimental Results (Section 4)** reports further empirical evidence, including results on a standard CIFAR-100 class-incremental benchmark under the PROOF setting and per-domain performance curves on the ten Stage-Bench domains.
- **Generalized Stage-CIL Protocol (Section 5)** outlines a more general formulation of Stage-CIL beyond the two-stage case, showing how our design naturally extends to multi-stage or branching evolution graphs.

Our core framework has already been implemented. Upon paper acceptance, we will promptly release the complete source code, together with scripts for reproducing all experiments and constructing Stage-Bench.

B. Details of Stage-Bench

As stated in the main paper (Sec. 3.3), this section provides a detailed description of the **Stage-Bench** dataset. Stage-Bench spans ten domains, each containing 20 classes, with every class annotated with two ordered morphological stages: Stage-0 (initial) and Stage-1 (evolved). The benchmark comprises 18,895 images with a roughly 1 : 1 balance between stages, yielding 400 morphological stages. Fig. 8 provides concrete examples of stage definitions across the ten domains.

Data Sources and Web Collection. A majority of images in Stage-Bench are drawn from established public benchmarks (e.g., Food-101 (Bossard et al., 2014), VegFru (Hou et al., 2017), Flowers (Nilsback et al., 2008), Birdsnap (Van Horn et al., 2015), Pets (Parkhi et al., 2012), MVTec-AD (Bergmann et al., 2019)). For each domain, we first identified classes whose semantics naturally support a two-stage interpretation. When the original datasets lacked explicit stage labels, we constructed Stage-0 and Stage-1 using a combination of programmatic filtering and manual grouping of visually compatible subclasses. To increase diversity and balance classes, approximately 29.6% of the images were additionally collected from publicly accessible web pages using class- and stage-specific keyword queries. Images and annotations for the Insects domain were sourced from our private internal database. This subset will be made available to qualified researchers for non-commercial research use. Access will be provided upon formal request and approval, after which a private download link will be issued.

Stage Annotation and Quality Control. Stage labels were assigned in a rigorous two-step process. First, an initial annotator proposed a coarse split into Stage-0 and Stage-1 based on salient morphological changes. Second, a different annotator independently reviewed all images for each class–stage pair to confirm, correct, or remove samples. Disagreements were resolved by a senior annotator. This quality-control loop was guided by a detailed annotation guideline containing textual descriptions and visual examples for each stage to promote consistent labeling decisions. Any image that remained ambiguous was discarded. This procedure ensures that the Stage-0/Stage-1 split reflects clear, semantically meaningful transitions. We will release mapping files linking Stage-Bench images to their original dataset identifiers or source URLs, enabling full traceability.

Licensing and Ethical Considerations. Stage-Bench is intended solely for non-commercial research and educational use. Images from existing benchmarks inherit their original licenses; we provide download scripts rather than redistributing the

images themselves. For web-collected images, we only used content that was publicly accessible and manually filtered all images to remove personally identifiable information (PII). No personal, medical, or otherwise sensitive attributes are annotated. We will fully document data sources and usage constraints, and we ask downstream users to respect the original terms of use of all underlying datasets.

C. Introduction about Compared Methods

In this section, we present the details of the methods compared in the main paper. Each method utilizes the same pretrained model (PTM) to ensure a fair comparison. These methods and their core limitations under the Stage-CIL setting are enumerated as follows:

- **iCaRL**(Rebuffi et al., 2017): employs knowledge distillation and exemplar-based replay with a nearest-mean-of-exemplars classifier. When naively adapted to Stage-CIL, replaying initial-stage exemplars during later-stage training conflicts with the stage-isolated protocol and can distort the learned trajectory of each class, making it harder to maintain coherent class identity across stages.
- **L2P**(Wang et al., 2022c): integrates visual prompt tuning into class-incremental learning using a pre-trained Vision Transformer, maintaining a prompt pool and selecting prompts for each instance via key–query similarity. In Stage-CIL, repeatedly fine-tuning shared prompts on later stages can accumulate interference from evolving appearances, leading to chain-like knowledge decay across a class’s evolutionary stages.
- **DualPrompt**(Wang et al., 2022b): introduces general prompts and expert prompts on top of L2P to model task-invariant and task-specific information. Under Stage-CIL, sequential optimization of expert prompts without explicit constraints on stage continuity can cause progressive drift of early-stage representations, so the same class may not be recognized consistently after large morphological changes.
- **CODA-Prompt**(Smith et al., 2023): decomposes prompts into a bank of basis components and uses attention-based reweighting to adaptively compose instance-specific prompts. In our Stage-CIL protocol, this query-dependent composition is not explicitly conditioned on stage order, and the finite component bank tends to be dominated by frequently seen later stages, limiting its ability to represent large intra-class morphology gaps.
- **EASE**(Zhou et al., 2024b): trains distinct lightweight adapters for each task to form task-specific subspaces and uses a semantic-guided prototype complement strategy to synthesize old-class features in new subspaces. When applied to Stage-CIL, the similarity-based complement does not explicitly encode ordered morphological evolution, so synthesized features for early stages can misalign with heavily transformed later-stage appearances, causing interference between stages of the same class.
- **SimpleCIL** (Zhou et al., 2025a): constructs a prototype-based classifier using a frozen PTM, continually setting classifier weights to class-wise prototype features with cosine classification. In our Stage-CIL instantiation, the class prototype is always estimated from the currently observed stage, so later stages overwrite earlier ones in the classifier space, leading to severe forgetting of early-stage appearances.
- **MOS** (Sun et al., 2025b): introduces task-specific adapters for PTM-based CIL and employs adapter merging to mitigate parameter drift, together with a self-refined adapter-retrieval mechanism at inference. When directly reused in Stage-CIL, adapter selection is oblivious to the ordered stage structure, and merging multiple adapters across tasks can blur decision boundaries between markedly different stages of the same class.
- **PROOF** (Zhou et al., 2025b): keeps the vision–language encoders (e.g., CLIP image/text backbones) frozen and incrementally adds task-specific projection heads plus a projection-fusion module to leverage multi-modal cues. In Stage-CIL, treating different stages of a class as separate tasks yields distinct projections per stage, which improves inter-task separation but does not explicitly enforce a shared identity manifold across stages, limiting its ability to model structured intra-class evolution.
- **S-Prompts** (Wang et al., 2022a): learns a pool of domain-specific prompts and retrieves the most relevant one for each instance using feature-based similarity search, originally for domain-incremental learning. When adapted to Stage-CIL by treating each morphological stage as a domain, this retrieval-based design captures domain selection rather than ordered evolution, and therefore fails to exploit the temporal and semantic correlation between evolutionary stages of the same class.

- **DCE** (Li et al., 2025): employs frequency-aware expert networks and a dynamic expert selector to handle imbalanced domain-incremental learning by routing inputs to specialized expert groups. Under Stage-CIL, instantiating stages as domains tends to allocate different stages of a class to separate experts, which weakens the modeling of a continuous evolutionary trajectory and may fragment a single class identity across multiple, loosely connected components.

D. Additional Analysis of STAGE

D.1. Pattern-Pool Dynamics

To better understand how STAGE exploits its evolution patterns over time, we analyze the usage statistics of the pattern pool during training. Concretely, for each pattern in the pool, we record its selection frequency (i.e., how often it appears in the **top- k** set) and compute the empirical distribution of frequencies across all patterns at different training stages. As illustrated in Fig. 10 and Fig. 11, the pattern pool exhibits a characteristic three-phase evolution behaviour that we summarize as *uniform* \rightarrow *differentiation* \rightarrow *re-balancing*.

In the early *cold-start phase*, pattern parameters are close to random initialization. As a result, different patterns have similar **cosine similarity scores** to the class anchors, leading to similar probabilities of being selected into the top- k set. The variance of usage frequencies remains low, and the pool behaves like an unstructured memory: no pattern has yet specialized to any particular morphology change.

In the *differentiation phase*, a subset of patterns receives more gradient updates (via the EMA-style update in Eq. (8) of the main paper) due to stochastic selection and early task exposure. These patterns are updated to better approximate true evolution vectors and therefore become **more likely to be selected again** by the top- k mechanism. This creates a “rich-get-richer” effect. Empirically, we observe a sharp increase in the variance of usage frequencies and the emergence of a small number of high-frequency patterns that dominate predictions for many samples. This phase corresponds to the pool discovering reusable evolution directions shared across classes and domains.

In the final *re-balancing phase*, two mechanisms jointly prevent the pool from collapsing onto a few patterns: (i) new classes and domains continuously introduce fresh gradients for previously unseen morphology changes, encouraging underused patterns to specialize; and (ii) the moving-average update of class anchors gradually shifts the reference points for evolution, making over-specialized patterns less universally optimal. Together, these factors allow underutilized patterns to be selected more often, while dispersing the dominance of saturated patterns and reducing the usage variance again.

Overall, this three-phase dynamics shows that the pattern pool in STAGE does not degenerate into a single dominant direction. Instead, it adaptively redistributes capacity over the course of training, maintaining a diverse set of evolution patterns within a fixed-size memory while remaining fully consistent with the hard top- k retrieval mechanism used in the main paper.

D.2. Computational and Memory Complexity

We next analyze the computational and memory overhead introduced by STAGE on top of the frozen CLIP backbone. All methods in the main paper share the same ViT-B/16 encoder; the additional cost of STAGE therefore comes solely from feature-level operations related to pattern retrieval and evolution prediction. As reported in Fig. 9, STAGE incurs a moderate overhead compared with strong PTM-based CIL baselines, while remaining in the same order of magnitude in terms of total training time.

Formally, let d denote the feature dimension, C the total number of classes seen so far, K the **total number of patterns in the shared pool** (i.e., the pattern-pool size; $K=50$ in our main setup), and k the number of patterns selected for each sample (i.e., top- k , with $k=5$ by default). For an input feature $f \in \mathbb{R}^d$, STAGE first computes similarity scores between f (or its corresponding anchor) and all K patterns in the shared pool to find the top- k , which costs $\mathcal{O}(Kd)$ operations. It then applies a small evolution network $E(\cdot)$ (implemented as a 3-layer MLP with hidden width h) to the selected patterns and anchor features, which costs on the order of $\mathcal{O}(kdh)$. Thus, the additional per-sample time complexity over the backbone forward pass is dominated by

$$\mathcal{O}(Kd + kdh), \quad (13)$$

which is negligible compared with the FLOPs of the ViT-B/16 encoder, since K , k , and h are modest constants in our experiments.

Table 3. Results on CIFAR-100 (B-0 Inc-10). All methods use the same backbone and weights

Metric	DualPrompt	SimpleCIL	PROOF	STAGE
\bar{A}	79.07	84.15	86.70	88.32
A_B	70.06	76.63	79.05	81.21

The main memory overhead of STAGE arises from storing class anchors and the **single shared pattern pool**. Anchors require $\mathcal{O}(Cd)$ memory, scaling linearly with the number of classes. The pattern pool requires $\mathcal{O}(Kd)$ memory, which is **constant** with respect to the number of classes. The total memory overhead can therefore be written as

$$\mathcal{O}(Cd + Kd), \quad (14)$$

which is small relative to the parameters and activations of the backbone. Overall, STAGE behaves as a thin, feature-space adapter on top of a frozen PTM, adding only lightweight computation and memory while enabling explicit modeling of morphological evolution.

E. Additional Experimental Results

E.1. Results on a Standard CIL Benchmark

To verify that the components designed for Stage-CIL do not **negatively impact** performance on standard benchmarks, we evaluated STAGE on CIFAR-100. The goal of this experiment is not to claim SOTA on standard CIL, but to ensure that our architecture does not “overfit” to the evolution-aware task.

As shown in Table 3, STAGE remains **highly competitive** on this standard benchmark, achieving performance slightly better than strong baselines such as PROOF. This result confirms that our predict-then-classify paradigm, even when morphological evolution is absent, **remains a robust CIL framework**. The added components are not detrimental to standard inter-class separation, validating the generality of our design.

E.2. Per-Domain Performance on Stage-Bench

To evaluate the behaviour of STAGE across diverse morphological evolution scenarios, we conduct separate incremental learning experiments on each of the ten domains in Stage-Bench. As Figure 12 shows, we compare STAGE against eight competitive methods from the main paper and visualize their performance curves across the two class-incremental steps for each domain.

Across all domains, STAGE consistently maintains the highest or near-highest accuracy at both incremental steps, and exhibits the smallest performance degradation as the number of morphological stages increases. The gains are especially visible in domains with pronounced appearance changes, where conventional CIL methods suffer from severe drops when moving from Stage-0 to Stage-1. These per-domain results support our claim that explicitly modeling intra-class evolution enables STAGE to remain robust under heterogeneous, class-specific morphology changes instead of relying on dataset-level averaging effects.

F. Generalized Stage-CIL Protocol

For completeness, we note that Stage-Bench corresponds to a special case of Stage-CIL with a two-node linear evolution graph. In general, each class c can be associated with a directed acyclic graph (DAG) of morphological stages $\mathcal{G}_c = (\mathcal{V}_c, \mathcal{E}_c)$, where nodes $s \in \mathcal{V}_c$ represent stages and edges $(s \rightarrow s') \in \mathcal{E}_c$ encode feasible transitions. Our current benchmark instantiates the simplest chain with $\mathcal{V}_c = \{0, 1\}$ and $\mathcal{E}_c = \{0 \rightarrow 1\}$ for all c . Thanks to its pattern-pool based evolution module, STAGE can be extended to multi-stage or branching graphs by applying the same predict-then-classify scheme along edges $(s \rightarrow s')$, which we leave as future work.



Figure 8. Illustration of Stage-Bench dataset. Each row shows one class across two morphological stages: Stage-0 (left block, initial form) and Stage-1 (right block, evolved form)

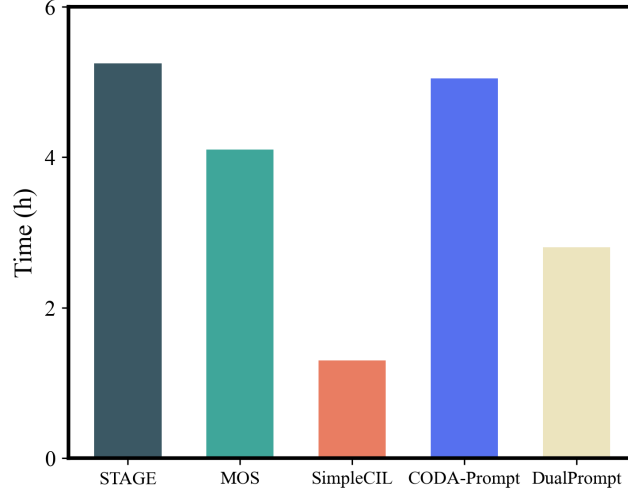


Figure 9. Running time comparison of different methods over Stage-Bench.

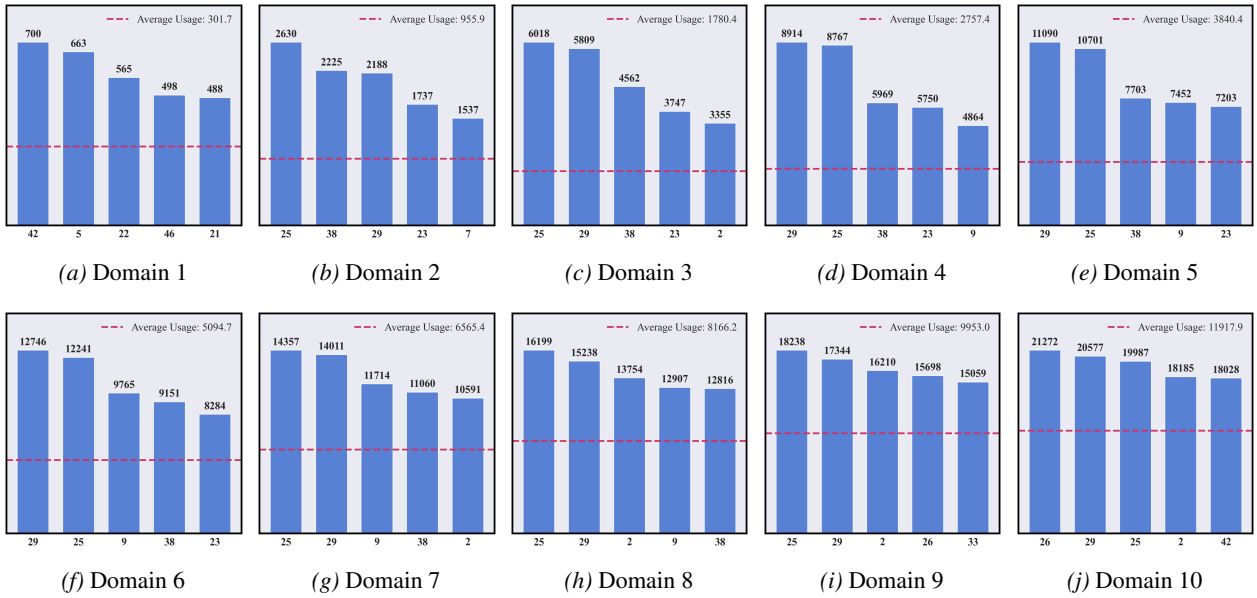


Figure 10. Evolution of pattern usage across Stage-Bench domains. Each subfigure displays the top-5 most frequently used evolution patterns after completing the corresponding domain.

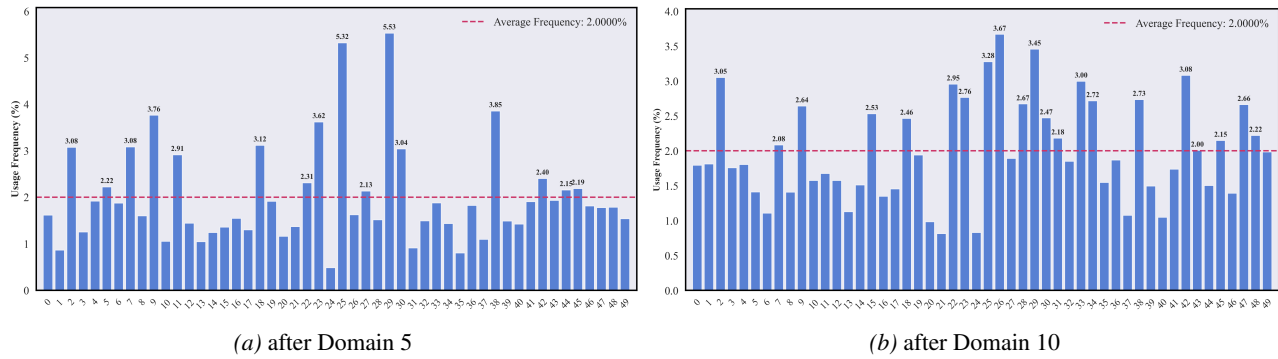


Figure 11. Pattern usage distribution evolution: Domain 5 (left) shows high variance with pattern monopolization, while Domain 10 (right) demonstrates balanced distribution through competitive updates.

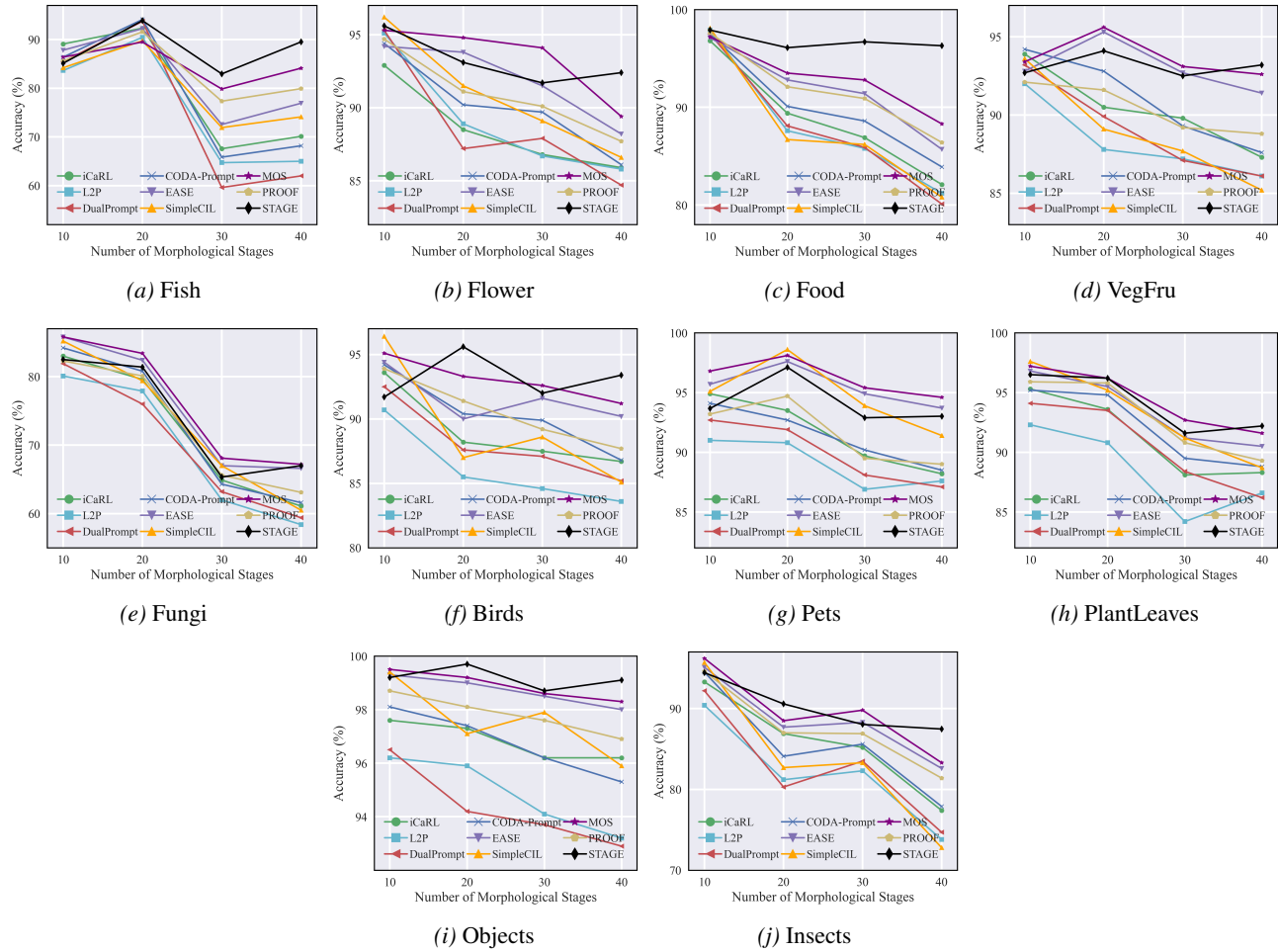


Figure 12. Performance curves of different methods across various domains of Stage-Bench. All methods use the same backbone and weights.